Smart Structures and Systems, *Vol. 24, No. 1 (2019) 37-52*
DOI: https://doi.org/10.12989/sss.2019.24.1.037

Overview of the development of smart base isolation system featuring magnetorheological elastomer

Yancheng Li[1,2] and Jianchun Li[*2,3]

[1]*College of Civil Engineering, Nanjing Tech University, Nanjing 211800, China*
[2]*School of Civil Engineering and Environmental Engineering, University of Technology Sydney, Ultimo, NSW 2007, Australia*
[3]*Tianjin Key Laboratory of Civil Structure Protection and Reinforcement, Tianjin Chengjian University, Tianjin, 300384, China*

(Received August 11, 2018, Revised February 22, 2019, Accepted February 27, 2019)

Abstract. Despite its success and wide application, base isolation system has been challenged for its passive nature, i.e., incapable of working with versatile external loadings. This is particularly exaggerated during near-source earthquakes and earthquakes with dominate low-frequency components. To address this issue, many efforts have been explored, including active base isolation system and hybrid base isolation system (with added controllable damping). Active base isolation system requires extra energy input which is not economical and the power supply may not be available during earthquakes. Although with tunable energy dissipation ability, hybrid base isolation systems are not able to alter its fundamental natural frequency to cope with varying external loadings. This paper reports an overview of new adventure with aim to develop adaptive base isolation system with controllable stiffness (thus adaptive natural frequency). With assistance of the feedback control system and the use of smart material technology, the proposed smart base isolation system is able to realize real-time decoupling of external loading and hence provides effective seismic protection against different types of earthquakes.

Keywords: smart base isolation; magnetorheological elastomer; adaptive base isolator; shake table testing

1. Introduction

Base isolation, one of the most widely accepted and applied seismic protection techniques, mitigates the effects caused by hazardous earthquake events by decoupling the superstructure from ground motion (Tiong *et al.* 2017). Since it is the transverse wave of the seismic motion that jeopardise the structural elements and building contents (Lu *et al*. 2011), the base isolation system provides lateral flexibility to the building to lower the stiffness of the link between the building and ground. As a result, the natural frequencies of the isolated structure are shifted by base isolation system and thus energy transmitted into the superstructure can be greatly reduced (Tiong *et al.* 2017).

Practical base isolation design is achieved through the optimisation depending on designated superstructure, type of the soil or foundation, historical earthquake characteristics, etc. Such optimisation, on the other hand, compromises certain required parameters in order to seek for robust performance of the system. For instance, the near-fault seismic activities, which features intense long-period velocity waves (usually with an amplitude of 0.5m/sec and period range between 2-4sec) (Ozbulut e*t al.* 2016), can be detrimental and induce excessive displacement response in the conventionally base-isolated structures with a period in this range (Lu and Lin 2009). One approach to allocate large displacement is to use larger base isolator, quite commonly implemented in Japan, which is effective but not economical (Tiong *et al.* 2017). Another usual approach is to use high damping isolator, i.e., high damping rubber bearing (HDRB) and New Zealand (or lead core) rubber bearing or additional viscous dampers in the base isolation system. However, high damping system that can cope with large displacement may cause large acceleration response and be less effective under moderate earthquakes (Jangid and Kelly 2001). The addition of damping, although reduces displacement, is at the expense of increasing the internal motion of superstructure (normally shown as inter-storey drift) as well as absolute accelerations. As known, minimising the structural acceleration and displacement is recognised as an irreconcilable conflict, of which displacement indicates structural damage while acceleration introduces condensed damage to the non-structural elements (Lu *et al.* 2011). Hence, it is beneficial if there is a type of base isolator that can adjust itself real-timely for optimal performance at each time instant without compromising either or both of the acceleration and inter-storey drift responses. Additionally, audience of the classic elastomeric base isolation is hampered to low- to medium-rise, more rigid buildings, as a result of possible uplifting forces in the isolators when the superstructure is tall and slender. The reason behind such limitation lies in that, if the building is tall enough, the horizontal acceleration of each floor will produce inevitable overturing moment and thus potentially produce tension in the isolation system.

To address these issues, researchers started seeking solutions from perspective of "smart" base isolation system combining passive base isolation system with controllable

*Corresponding author, Dr.
E-mail: Jianchun.li@uts.edu.au

ISSN: 1738-1584 (Print), 1738-1991 (Online)

active or semi-active damping devices (Yoshioda *et al.* 2002). The most popular semi-active damping device is magnetorheological (MR) damper which features tuneable viscous damping in the presence of a varying magnetic field (Yoshioda *et al.* 2002). In the disciplines of structural control, such isolation system should be categorised as hybrid control system. The hybrid control strategy has been proved to be effective in terms of seismic protection throughout comprehensive numerical and experimental testings (Yi *et al*. 2001, Dyke *et al.* 1996, Yoshida and Dyke 2004, Nagarajaiah and Narasimhan 2006). However, the role of damping in seismic isolation has been comprehensively studied by Kelly (1999) and results demonstrate that use of supplementary dampers in seismic isolation is a misplaced effort and will cause undesirable side effects. It is well known that damping is able to primarily control vibration responses under the circumstances of steady-state resonance and free vibration stage. Nevertheless, when confronted with impact load, which is particularly featured in near-fault earthquakes, not enough time is allowed for the damping to dissipate vibrational energy. Since the hysteresis nature of damping is not changed, it is worth questioning whether or not the semi-active or "smart" damping can cope with the sudden change in external load or structure. Moreover, despite the fact that the supplementary damping may forcefully confine the base displacement of the passive base isolation system (Tiong *et al*. 2017), high-frequency accelerations as well as increase of inter-storey drifts may be introduced to the superstructure by augmenting damping (Li *et al*. 2013a).

To achieve real-time optimal base isolation, researchers have been seeking the development of another type of smart base isolation system by using controllable stiffness device, i.e. base isolator. With real-time controllable lateral stiffness of the base isolator, the base isolation system is able to instantaneously shift the fundamental natural frequency of the base-isolated structure and therefore the optimal base isolation scenario can be fulfilled with the assistance of the feedback system and control unit. one of the examples is the utilization of smart rubber material, i.e., magnetorheological elastomer, to develop smart base isolator and smart isolation system.

Magnetorheological (MR) elastomer is a relatively new addition in MR material family, whose shear modulus and damping can be changed by magnetic field in real-time (Li *et al.* 2012, Li *et al.* 2010). It is normally a compound material with polarizable particles suspended in a non-magnetic solid or gel-like matrix, which is mixed with silicone rubber and silicone oil. Typically, during the process of curing magnetic field is applied to the mixture so that the chain-like structure can be formed and fixed in the matrix after the curing. When the process is completed, MR elastomer is similar to a soft rubber with the absence of magnetic field. However, under magnetic field, the elastic modulus of MR elastomers can be increased greatly depending on the strength of the magnetic field and the designed property of MR elastomer (Li *et al*. 2014). Utilizing the unique field-dependent material properties, a smart base isolator has been designed and prototyped with inherited laminated MR elastomer and steel structure (Li *et al.* 2013), which can be used to develop the smart base isolation system.

In this paper, an overview of the recent development of the smart base isolation system is given. Firstly, the concept of the smart base isolation system is proposed for discussion. The key technological developments are introduced, including the device design and characterisation, nonlinear hysteresis modelling, structural control algorithm, experimental validation. Finally, a discussion on the challenges faced is presented in regard of the future development or possible applications.

2. Smart base isolation system

A smart base isolation system should be able to realize the real-time decoupling of ground motion and thus provide optimal seismic protection to the structures under multiple types of earthquakes. The methodology is through controlling the isolator's lateral stiffness in real time and hence decouple the superstructure from ground motion at any time instant according to the characteristics of the upcoming earthquake as well as the structural responses.

Fig. 1 compares the schematics of three types of base isolation systems, i.e. the traditional base isolation with passive damping, the hybrid base isolation which equips passive isolator with active or semi-active damper, the smart base isolation system with stiffness-controllable base isolator. Both hybrid base isolation and smart base isolation system employ a sensing network, signal processor and control decision unit. However, the control effect is applied on the structure differently, i.e., in hybrid base isolation system, the control action is applied in the form of damping force while in smart base isolation system, while in the smart base isolation system, the control effect is realized by altering the lateral stiffness of the base isolator. By controlling the isolator's stiffness, the natural frequencies of the smart base isolation system are shifted away from dominant frequency components of the earthquake excitation and hence a non-resonant state is achieved at every moment. Therefore, the proposed smart base isolation system can manage to attain a superior seismic protection performance.

Fig. 2 illustrates the essential configuration of a smart base isolation system. The realisation of the concept features four key parts:

i) Stiffness-controllable smart isolator: the stiffness controllable base isolator should be able to provide instantly controllable lateral stiffness to enable real-time decoupling from the ground motion. Hence, the proposed smart base isolation system should be categorized as a semi-active control system and the adaptive isolator is the indispensable key to realize such concept.

ii) Properly designed and representative structure model: as a testing bed, the scaled structure model should manage to represent typical low- to mid-rise buildings. Meanwhile, the designated fundamental frequency should fall in the range of dominant frequency of common earthquakes to highlight the contracting seismic response between bare building and base-isolated structure.

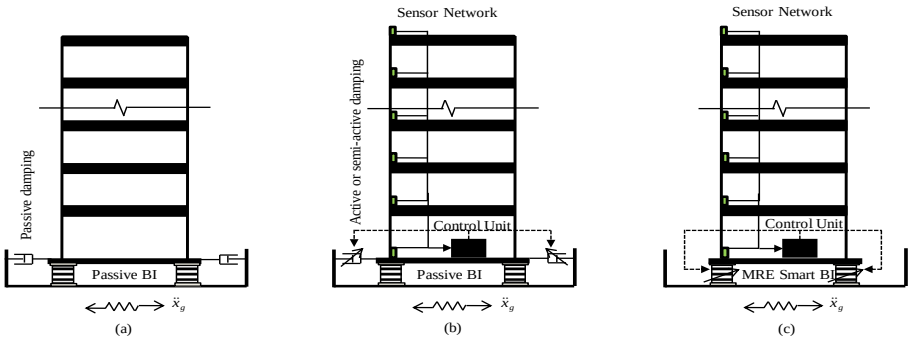

Fig. 1 Schematic diagram of (a) traditional base isolation system, (b) hybrid isolation system combining passive base isolation with active or semiactive dampers and (c) smart base isolation system with MR elastomer base isolators (BI: base isolation)

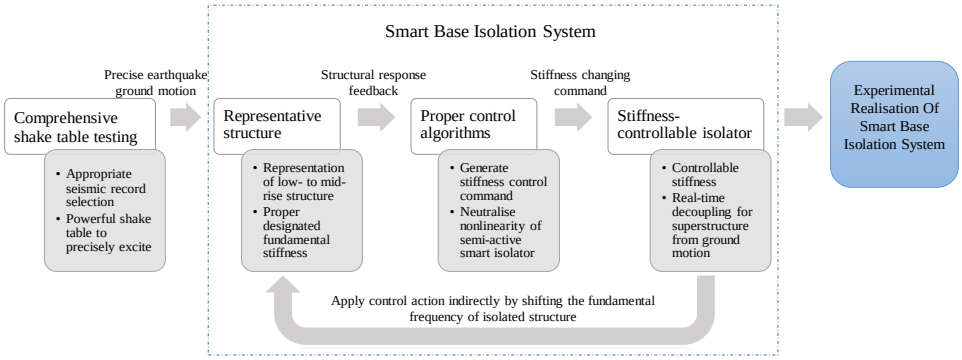

Fig. 2 Basic configuration of a smart base isolation system

iii) Appropriate control algorithm: as known, the smart base isolator is a semi-active control device which influences the response of isolated structure by altering its lateral stiffness so the controller should be developed to generate stiffness-changing command instead of simply calculating desired control force. Moreover, due to the inherent hysteretic dynamics of the semi-active isolator, the control strategy should be able to bear or cope with the nonlinearity of the control system to avoid performance degradation or system instability.

iv) Comprehensive shake table testing: the selection of earthquake excitation collection should celebrate a diversity including both far- and near-fault earthquake to demonstrate the versatility of proposed smart base isolation system and the experiment should be conducted on a powerful shake table to ensure the earthquake inputs' intensity and developed, and some of them have been implemented into seismic protection of lab-scaled buildings. Kobori *et al.* (1993) proposed an active variable stiffness device to establish non-resonant state against the earthquake excitations. The active variable stiffness device comprises a double-ended enclosed hydraulic cylinder and a regulated valve inserted in the cylinder to realize two stiffness states, i.e., "locking" and "unlocking". The device served as brace in the building to regulate the structural stiffness. Switching between on-off states can alter structural stiffness and the system developed performed successfully to combat with several earthquakes. However, the sudden change between two states may introduce undesirable acceleration into the accuracy.

3. Technological development

3.1 Design of smart base isolator with real-time controllable lateral stiffness

3.1.1 Historical development

The adaptive base isolator with capacity to, which may be subjected to external stimuli, alter its lateral stiffness in an instantaneous, reversible and controllable manner serves as cornerstone of the development of the smart base isolation system. Using the concept of variable stiffness to develop adaptive base isolation system has been pursued by the community since the past few decades. A number of variable stiffness devices have been proposed and developed, and some of them have been implemented into seismic protection of lab-scaled buildings. Kobori *et al.* (1993) proposed an active variable stiffness device to establish non-resonant state against the earthquake excitations. The active variable stiffness device comprises a double-ended enclosed hydraulic cylinder and a regulated valve inserted in the cylinder to realize two stiffness states, i.e., "locking" and "unlocking". The device served as brace

in the building to regulate the structural stiffness. Switching between on-off states can alter structural stiffness and the system developed performed successfully to combat with several earthquakes. However, the sudden change between two states may introduce undesirable acceleration into the building and thus create harmful effect to sensitive equipment and occupants. Enlightened by this, Narasimhana and Nagarajaiah (2005) proposed a semiactive variable stiffness device which is capable of providing smooth stiffness variation along x or y direction. It has been proved to be able to reduce storey drift and storey acceleration simultaneously. However, such design limits its motion in single direction which may jeopardise its applicable areas. Emergence of the smart material technology embraces great potential in developing high efficiency variable stiffness isolation devices. Makris (1997) opened a discussion on how the electrorheological (ER) dampers can be used to protect the base-isolated structures against near-fault earthquakes. Conclusion drawn from his research suggests that carefully designed ER damper with friction-force dominance can reduce the storey displacement while maintaining low level acceleration. The conclusion also applied to the MR damper. The special requirement on the ER/MR damper design imposes great challenge in its applications.

On the other hand, MR elastomer becomes a favourite candidate due to its distinctive material features, such as large/smooth stiffness variation, real-time controllability and rapid response time. Usman *et al.* (2009) numerically evaluated the dynamic performance of a smart base isolation system employing MR elastomer, and the results show that the proposed system outperforms the conventional system in reducing the responses of the structures during seismic excitations. Based on the performance of MR elastomer, Jung *et al.* (2011) investigated the behavior of a small-scale, single-story building structure incorporated with MR elastomers. The results show that the proposed MR elastomer base isolation system with the fuzzy logic control algorithm outperforms the conventional passive-type base isolation system in reducing the responses of the building structure for the seismic excitations. Those researches proposed the idea of using MR elastomer to develop smart base isolation system. However, the essential device, e.g. the base isolator, has not been designed and the development was still in the very early stage. The classical structure for rubber bearing, i.e. laminated rubber and steel combination, was not incorporated into the smart base isolator design.

3.1.2 Structure of the adaptive MR elastomer base isolator

Li *et al.* (2012, 2013a, b, c) successfully prototyped the first laminated base isolator using MR elastomer. The configuration of the novel MR elastomer base isolator, as shown in Figure 3, incorporates the laminated structural design of traditional laminated rubber bearing. It consists of multilayer thin MR elastomer sheets bonded onto multilayer thin steel plates. The laminated structure is essential for the seismic isolator used in civil engineering applications. It provides large vertical load capacity and stiffness, and prevents lateral bulging and malfunctioning of the MR elastomer rubber. The laminated structure allows high flexibility in horizontal direction by the shearing deformation of MR elastomer sheets that can also be varied instantly under applied magnetic field. In this design, there are 24 layers of the steel sheet with thickness of 1 mm and 25 layers of MR elastomer sheets with thickness of 1 mm being used. The diameter of the MR elastomer and steel sheets is 120 mm.

In the design, the laminated bearing element is placed inside of a solenoid, which generate uniform magnetic field after it is energized with electric current (Li *et al.* 2013a, Li *et al.* 2013c). The solenoid is made of electromagnetic coil and thin non-magnetic support as illustrated in figure 3. The cylindrical shape non-magnetic support is made of epoxy material and has an inner diameter of 146 mm. The thickness of the thin wall is 2 mm. The cylindrical electromagnetic coil has an inner diameter of 150 mm and an outer diameter of 200 mm. The coil is firmly attached to the epoxy support. The diameter of the coil wire is 1.0 mm with a total winding number of 2900 turns. The wire made of copper has electric resistance of 42.3 Ω. Thus, under a full scale electric current of 3A, the power consumption is approximately 370W. The space between the laminated MR elastomer structure and the surrounding coil allows the MR elastomer isolator to a maximum displacement range of ±15 mm, equivalent to the maximum allowable shear strain of 60%.

The vertical load carrying capacity of the MR elastomer isolator is 50 kg under maximum designed shear displacement (i.e., 15 mm) and zero magnetic field. When the shear displacement is less than 15 mm, the vertical loading capacity of the device will be greatly enhanced. As the loading capacity is a function of cross-sectional area, thickness and the shear modulus of MR elastomer layer, it can be designed based on the requirements of applications.

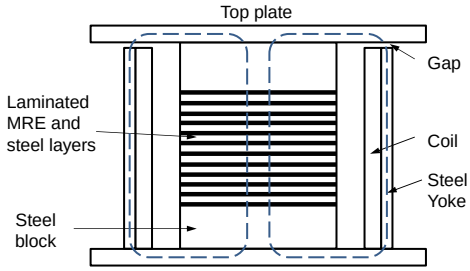

(a) Sketchmatic of the adaptive base isolator

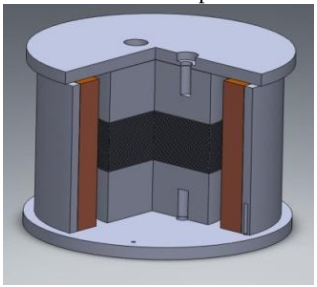

(b) 3D illustration

Fig. 3 The laminated MR elastomer base isolator

Table 1 Final current and force response time (4mm displacement, field-quenching configuration)

	Current measurement		Force measurement	
Response time (ms)	Rising	Falling	Rising	Falling
	44	40	52	48

The MR elastomer material used in this design was expected to produce 15 times increase on shear modulus under magnetic field (Li *et al.* 2013c). With the given device design, the experimental results showed more than 15 times of the stiffness increase were achieved.

3.1.3 Magnetic design

Unlike the designs of other MR elastomer devices, in this design the MR elastomer materials are placed inside the coil. According to the principle of magnetics, all the magnetic lines that enter any region must also leave that region. In a magnetic circuit, the area inside the coil is the region that all magnetic lines must pass through. Therefore, this placement guarantees uniform and strongest magnetic field given sufficient magnetic flux is provided. Laminated MR elastomer structure with steel layer embedded serves as part of the magnetic core. The magnetic conductivity of the MR elastomer material is fairly low due to the large volume fraction of rubber matrix and hence to achieve saturated magnetic field for MR elastomer material considerable power consumption is expected. Laminated structure with high magnetic conductive steel layers between MR elastomer layers improves its overall magnetic conductivity. Two solid steel blocks are added on the top and bottom of the laminated structure to further improve the permeability of the magnetic core. To form an enclosed path for the magnetic flux, two steel plates, one on the top and the other on the bottom, are designed to perform two roles as: 1) creating paths for magnetic field and 2) being fixture to connect the device to the ground and the superstructure above (Li *et al*. 2013 a). In addition, an annular steel yoke is attached to the coil to complete the magnetic flux path. Gap between the top connection plate and the steel yoke allows lateral deformation of base isolator. Size of the gap is determined by considering the compression of MR elastomer layers under maximum designated compressive loading and stability under maximum lateral deformation.

Finite element analysis was conducted using ANSYS Maxwell software. Magnetic property of the MR elastomer material was obtained from the testing setup used in Zeng *et al.* (2013). Other parts of the device, including annular yoke, steel plates, steel sheets and steel blocks, are all made of steel 1008. The magnetic property of the steel can be found in the software.

Fig. 4 shows the magnetic flux density inside of the device when applied current is 3.0A. It can be observed that the magnetic field inside of the MR elastomer material is around 0.9 T and the distribution is uniform for all MR elastomer materials. Li *et al*. (2013d) has demonstrated that the magnetic field in a solenoid reaches highest in the center, while it gradually weakens when leaving the center due to the dispersion of the field. Built on this, the laminated MR elastomer and steel structure was designed in the center of the magnetic core, while high permeable steel blocks was attached to the laminated structure. This arrangement can shift the weakening magnetic field away from the MR elastomer materials. Due to the better conductivity, the magnetic field inside other narrow magnetic paths, i.e., connecting plates and yoke, is much stronger than that in MR elastomer material. This is not a surprise since the magnetic conductivity of MR elastomer material is much lower than steel. However, laminated structure with alternative steel sheets and MR elastomer sheets greatly improves the magnetic permeability of the structure as a whole (Li and Li 2015a).

3.1.4 Response time optimization

To be successfully implemented in the structural control system, the MR elastomer base isolator should possess instant response on the lateral stiffness under control signal. However, the design of MR elastomer devices usually adopts larger electromagnetic coils thus complex design of driving electronics is inevitably required for the device, which creates obstacle to achieve a fast response time. To address this issue, two methods are used to design the electromagnetics of the MR elastomer isolator. Firstly, the coil used in the design consists of a number of small coils connected in parallel which can greatly reduce the response time of the device. For example, if n identical coils are in parallel connection to generate same level of magnetic field of the original coil, its response time is 1/n of the original response of the original coil. In addition, PWM switch and field-quenching arrangement are also adopted in the coil design, with details can be found at Gu *et al. (*2016).

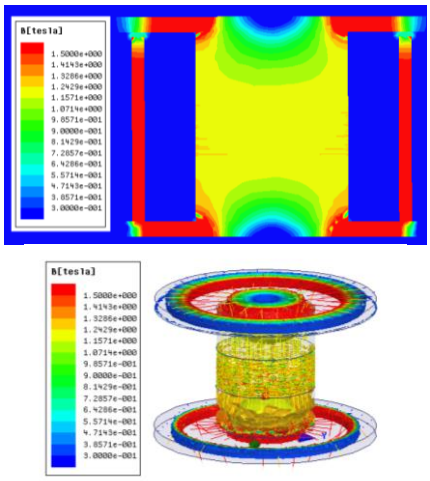

Fig. 4 Magnetic flux density when current I =3.0A: 2D model and 3D model

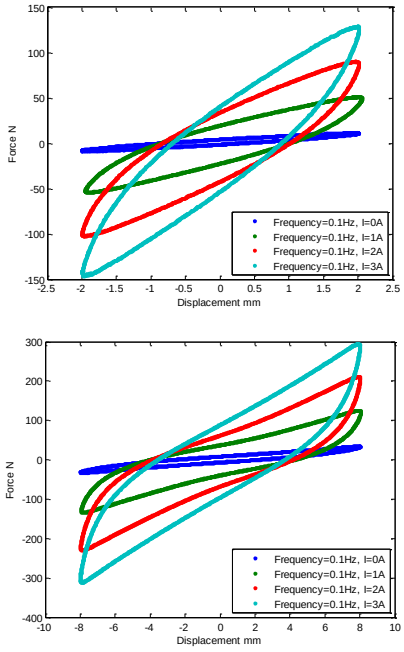

Fig. 5 Force-displacement relationships of the MRE base isolator at quasi-static testing with frequency of 0.1 Hz (Δ=2 mm and 8 mm)

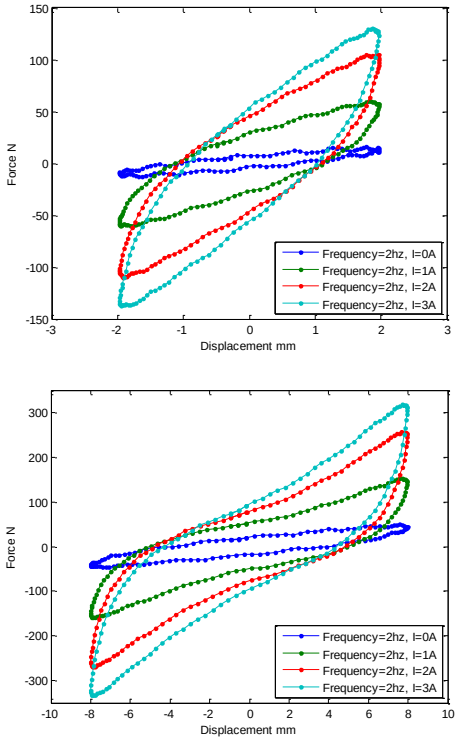

Fig. 6 Force-displacement relationships of the MRE base isolator at quasi-static testing with frequency of 2 Hz (Δ=2 mm and 8 mm)

The field quenching is to remove the magnetic field residual which further reduces the response time. Tables 1 gives the response time of final design of the MR elastomer base isolator. As observed, the response time has been greatly reduced from 421 ms to 52 ms for rising edge and from 402 ms to 48 ms for falling edge. Such response time makes the real-time control feasible.

3.1.5 Device performance

Figs. 5 and 6 show the force-displacement loops of the MRE base isolator at various sinusoidal loadings of three amplitudes at frequencies of 0.1 Hz and 2.0 Hz, respectively. For each loading case, force increases with applied currents can be clearly observed. The measured force also increases with increase of the loading amplitude naturally. Since the slope of the force-displacement loops indicates the lateral stiffness of the MR elastomer isolator, it can also be observed that at certain current range the stiffness of the MR elastomer base isolator gains considerable larger increase. Moreover, as the enclosed area of the loop represents the energy dissipation, or the damping equivalent, of the MR elastomer isolator, it is noted that the damping of the MR elastomer isolator increases when the applied current increases.

It is found that the maximum stiffness increases of the MR elastomer isolator can reach 1630% at low amplitude quasi static excitation. With the increase of the loading amplitude, the stiffness increase declines, which should attribute to the variation of the chain structure in the MR elastomer material (Li *et al.* 2013 c).

It should be pointed out that the present design aims to explore maximum capacity of MR effect, in terms of stiffness change, without considering the temperature impact on the coil, i.e., the overheating issue. A trade-off between MR effect and temperature in the sustainable operations can be considered in the design if a practical application is to pursuit. Chen *et al*. (2016) has conducted an optimal design of MRE isolator integrating the MRE material design into mechanical and electromagnetic components to achieve a trade-off between power consumption and adjustability of stiffness.

3.2 Nonlinear modelling of the hysteresis behavior of the base isolator

Establishing accurate model of the MR elastomer base isolator is an essential task to reproduce the nonlinear device behavior and to lay foundation for its control applications. Till now, several models have been proposed to describe the complex behavior of the MR elastomer base isolator, including parametric models and non-parametric models.

Regardless the type of the model, the modelling process normally involves two steps: firstly, the proposed model is trialed by standard sinusoidal loadings with various loading amplitudes, loading frequencies and applied currents; After this step, a generalized model is obtained which should include the linearization process to establish the relationships between the model parameters and the applied currents. In the second step, the generalized model is to be tested by the output data of the device under randomized excitation and/or applied currents. This is due to the fact that the operating condition of the device is normally under

stochastic loadings and therefore the proposed model should be able to predict the behavior of the device under such condition.

3.2.1 Parametric models

As shown in the force-displacement loops in Figures 5-6, it is clear that the parametric model should at least consist of stiffness and damping elements, representing by the inclines slope and the size of the hysteresis loops. For a model with stiffness and damping elements only, the hysteresis loop is an inclined ellipse shape. However, there is nonlinear behavior existing in the loop and therefore the element with nonlinear hysteresis should be included in the model as well. To address this issue, several models have been proposed, such as Bouc-Wen model (Yang *et al.* 2013, Behrooz *et al.* 2014a, b), strain-stiffening model (Li and Li 2015b, Li and Li 2016, Yu *et al*. 2015a) improved LuGre model (Yu *et al.* 2015b), improved Dahl model (Yu *et al.* 2014), etc.

Yang *et al*. (2013) proposed a Bouc-Wen model to characterize the behavior of MRE base isolator, Fig. 7. This model consists of a spring, viscous dashpot and a hysteresis Bouc-Wen element in parallel, as following

$$\begin{aligned} F &= \alpha k_0 x + (1-\alpha) k_0 z + c_0 \dot{x} \\ \dot{z} &= A\dot{x} - \beta|\dot{x}||z|^{n-1} z - \gamma \dot{x}|z|^n \end{aligned} \tag{1}$$

k_0 is the stiffness of the spring, and c_0 represents the viscous coefficient, indicating the damping capacity of the system. The item of $c_0\dot{x}$ is a component of the total force. The rest part represents the restoring force as the summation of a linear component $\alpha k_0 x$ and a purely hysteretic component $(1-\alpha)k_0 z$, in which $\alpha \in (0,1)$ represents the linearity level of the hysteresis loops. A, n, β and γ, which are non-dimensional parameters, are responsible for the shape and the size of the hysteresis loops.

Yu *et al*. (2015b) proposed an improved LuGre model to characterize the behavior of MRE base isolator. The model consists of a spring element, a viscous dashpot and a modified LuGre element connected in parallel, with mathematical expression is given by

$$\begin{aligned} F(t) &= k_0 x(t) + c_0 \dot{x}(t) + \frac{\beta}{\alpha} y(t) + \frac{\varepsilon}{\alpha} \dot{y}(t) + f_0 \\ \frac{1}{\alpha}\dot{y}(t) &= \dot{x}(t) - |\dot{x}(t)| y(t) \end{aligned} \tag{2}$$

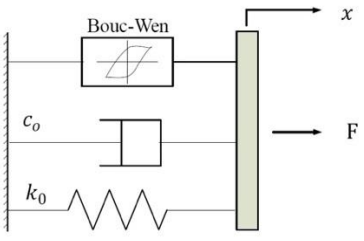

Fig. 7 Bouc-Wen model for the MR elastomer base isolator

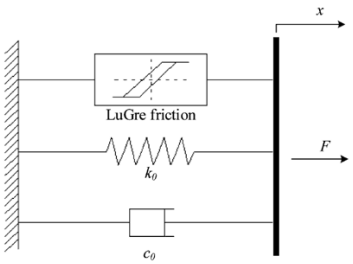

Fig. 8 Improved LuGre friction model for the MR elastomer base isolator

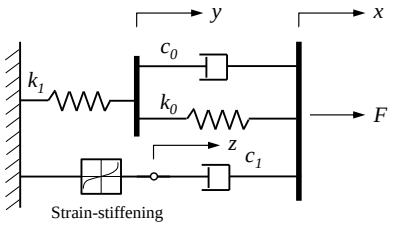

Fig. 9 Strain-stiffening model for the MR elastomer base isolator

where $F(t)$ is the shear force of the model output at time t; $x(t)$ and $\dot{x}(t)$ denote the displacement and velocity of the device at time t, respectively; k_0, c_0 and f_0 are the spring stiffness, viscous damping and initial force of the device, respectively; y is an intermediate variable; α, β and ε are three non-dimensional parameters, which are used to control the shape and scale of the hysteretic loop.

Li and Li (2015b, 2016) have proposed a strain-stiffening model, Fig. 9, with a hysteresis strain-stiffening element involved to characterize the behaviour of MRE isolator. The details of the model are as followings

$$\begin{aligned} F &= k_1 y + \alpha z^3 \\ k_1 y &= k_0 (x - y) + c_0 (\dot{x} - \dot{y}) \\ \alpha z^3 &= c_1 (\dot{x} - \dot{z}) \end{aligned} \tag{3}$$

Where, c_0, k_0, c_1, k_1 and α are the model parameters to be identified. This model contains a strain-stiffening element to portrait the nonlinear behaviour of the isolator. It also has a nominal displacement y in the standard solid model to be calculated, which may introduce extra computational efforts. To overcome this issue, a new strain-stiffening model has been proposed (Yu *et al.* 2016a), as shown in Fig. 10.

The mathematical expression of the proposed model is as followings

$$F = k_0 x + c_0 \dot{x} + \alpha |x| x^3 + F_0 \tag{4}$$

Where, k_0, c_0 and α are the model parameters as stiffness of the spring, damping of the dashpot and coefficient of the modified strain-stiffening element. F_0 is the offset of the shear force. Without the nominal displacement involved, the modified strain-stiffening model has simpler structure and only four model parameters are to be identified.

Table 2 Model performance comparison

Model	Number of model parameters	RMS error %	Running time s
Bouc-Wen	7	5.3194	168.4959
Improved LuGre friction	6	5.8728	151.6732
Strain-stiffening	5	5.6322	32.1143
Improved strain-stiffening	4	5.4935	2.7367

The listed models can reproduce the behaviour of the MR elastomer isolator very well under both sinusoidal loadings and randomized loadings. Table 2 compares the RMS errors and calculation time of different models after parameters are identified. The four models have similar RMS error, which show good model accuracy. Due to the variation of the model parameters included, the running time is quite different: Bouc-Wen model requires most computational resources while the improved strain-stiffening model demands the least. The reason lies in the number of model parameters and the complexity of the nonlinear hysteresis elements. In term of their applicability in the control design and analysis, Bouc-Wen model has proven popularity in this regard due to its explicit boundedness of the hysteresis part (Chen *et al.* 2018) while the strain-stiffening models have to face the challenge that they do not have boundedness in a pure mathematical point of view.

3.2.2 Non-parametric models

In the parametric models, all the model parameters possess physical meaning to explain the actual behavior of the device. For example, the stiffness element refers to elastic behavior of the device for which one can correlate to the inclined slope of the hysteresis loop. The damping coefficient links to the characteristic of viscous damping, usually represented by a dashpot, and the magnitude of the damping coefficient has direct relation with size of the enclosed loop. However, the model accuracy may be affected by limited choice of the model forms and sometimes meaningless values of the coefficients may be identified based on the experimental data, such as negative stiffness and damping.

Non-parametric models differ from parametric models as the model structure is not specified a priori or not pre-defined but is instead determined from data. This feature adds flexibility and consequently accuracy into the model. In the non-parametric modelling process of MR elastomer base isolator, the adopted methodology, such as neuro network, supporting vector, etc, establishes the relationship between the motion of the isolator (e.g., displacement, velocity, loading frequency and applied current) and the force output. The pre-set form of the parametric model utilizes current and previous states of responses to predict its output. The non-parametric model can capture more subtle aspects of the data and has higher accuracy and more freedom in the device modelling.

Several research have been reported to use non-parametric modelling technique to predict the nonlinear behavior of the MR elastomer base isolators. Koo *et al.* (2009) developed a phenomenological model to capture dynamic behaviors, i.e., stress-strain relationship under compressive loadings, of MR elastomers using artificial NN method. Yu *et al.* (2015c) proposed a feedforward NN and ant colony algorithm to model the behavior of laminated MR elastomer base isolator. Leng *et al.* (2018) established an artificial neuro network to model the behaviors of magnetorheological elastomer isolator in shear-compression mixed mode. Yu *et al.* (2016b) utilized support vector regression and particle swarm optimization/fruit fly algorithm, respectively, to reproduce the behavior of MR elastomer base isolator.

Fig. 10 illustrates the structure of a support vector regression (SVR) based model for MR elastomer base isolator (Yu *et al.* 2016b). In this nonparametric model, the displacement and velocity of the device, as well as the current, are adopted as the inputs, while the shear force of the device is regarded as the output of the model. It is shown in Fig. 11 that the SVR model can well predict the behavior of the MRE base isolator in all loading conditions, i.e., multiple loading frequencies and amplitudes.

Clearly, due to the flexibility, the non-parametric model performs better compared with parametric models. The non-parametric modelling technique is very popular to characterize the nonlinear behavior of devices and structures. It is yet to see its popularity to emerge in the structural control application compared with parametric models.

3.3 Structural control algorithms

The proposed smart bae isolation system works in a way to actively alter its lateral stiffness to achieve real-time decoupling of the external dynamic loading and thus offers the optimal protection of the civil structures (Chen *et al.* 2016, Yu *et al.* 2016). To accomplish this, the adoption of appropriate control algorithms is the key to provide accurate applied current to the electromagnetic coil under the motion condition of any given time instant. In the smart base isolation system, the base isolator introduces high hysteresis into the control loop, which should be addressed.

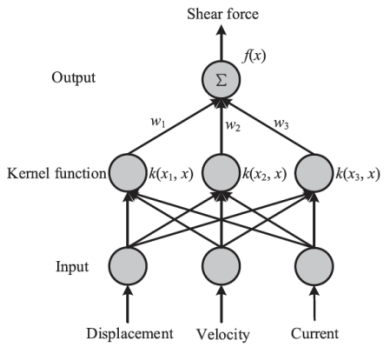

Fig. 10 Structure of a support vector regression based model

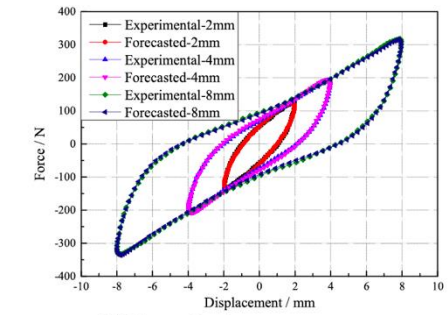

(a) Force-displacement responses

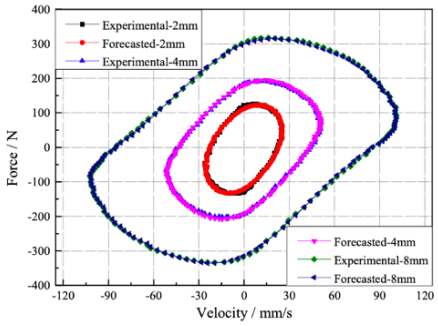

(b) Force-velocity responses

Fig. 11 Comparisons between experimental and forecasted data with different loading amplitudes

In this section, two control strategies adopted in the study of smart base isolation system, i.e., the classical Bang-Bang control (on-off) and GA optimized fuzzy logic control are presented. The GA optimized fuzzy logic control is to provide robustness to the control system which can be endangered by the hysteresis of the smart base isolator.

3.3.1 Bang-Bang control

The Bang-Bang control can also be implemented in the smart base isolation system. In this control design, the MR elastomer base isolator only provides two states, i.e., maximum stiffness (on state) and minimum stiffness (off state). The control algorithm switches the smart base isolator between on and off states based on the sensory feedback from the data acquisition system. The detailed control algorithm is as following

$$g(t) = \begin{cases} 1 & \dot{x}_b x_b > 0 \\ 0 & \dot{x}_b x_b < 0 \end{cases} \tag{5}$$

The switching principle of variable stiffness is related to the structural response x_b and variable $\dot{x}_b$. The own physical interpretation is as following: when the structure's displacement and velocity are with the same sign, which means the superstructure is moving away from the equilibrium position, the smart base isolator provide additional stiffness for the system; on contrast, when the displacement and velocity are with the opposite signs, which means the superstructure is moving towards the equilibrium position, the isolator maintains the softest situation (Gu *et al.* 2019).

3.3.2 GA optimised fuzzy-logic control

Because of the high nonlinearity and uncertainty of MR elastomer base isolated structure, the uncertain and imprecise of the isolation system is a significant issue in real experimental applications. It is well-known that the fuzzy logic control, which is not dependent on the synthesis and analysis of the mathematical control system (Gu *et al.* 2019), is quintessential for the control of the smart base isolation system and thus allows considerable nonlinearity and uncertainty of the input excitation, feedback signal and the controlled structure itself. The inputs and outputs of the fuzzy controller are described in linguistic directions and then connected by the fuzzy inferences of "IF-THEN" rules.

Normally, a well-designed base isolation system should be able to achieve small base drift and structural acceleration simultaneously. Thus the aim of the fuzzy logic controller designed in this study is to minimise the structural acceleration and base drift simultaneously (Gu *et al.* 2017, Gu *et al.* 2019). Top floor acceleration and base level displacement are then chosen to be the inputs of controller whose output is the control current of the MR elastomer isolator. The responses can be divided into three types: 1) when the absolute acceleration is very large, the base isolation should be soft enough to release the superstructure and thus dissipate energy when the base drift is small and vice versa; 2) when the absolute acceleration is small, the stiffness of the base isolation should be positive correlated to absolute base drift, which ensures the stability of the building; 3) when the absolute acceleration is around zero, the control current should be small when the base drift is big and big when base drift is almost zero, which will ensure high base stiffness without the existence of seismic excitation.

Specific control law was obtained and optimized by a non-dominated sorting genetic algorithm type II (NSGA-II). Dynamic crowding distance (DCD) is introduced into the standard NSGA-II as a novel evaluation index to keep good diversity among the solutions. More details about NSGA-II with DCD can be found in reference [45]. The peak and root mean square (RMS) of top floor acceleration and base drift are adopted to construct the fitness function. The optimized inference rule of the fuzzy logic controller is shown in Table 3. The member functions (MF) of the input signals are abbreviated as: PB = big positive; PM = medium positive; PS = small positive; Z = zero; NS = small negative; NM = medium negative; NB = big negative; while the MFs of output signals are: B = big; M = medium; S = small.

3.4 System integration: building model, power supply, sensory network, data acquisition and control system

Fig. 12 illustrates the detailed system description of a smart base isolation system featuring the MR elastomer isolators. The building (or building model, for a lab-scaled research), smart base isolators, sensor network, data acquisition system, control unit, power amplifier and power supply are the fundamental elements in the system. The building or building model should install a sensor network to monitor the building behavior in real-time. Usually,

Table 3 Optimized inference rule of the fuzzy logic controller

MF		Top floor acceleration				
		PB	PS	Z	NS	NB
Base Drift	PB	M	B	S	S	M
	PM	S	B	S	B	S
	PS	S	S	B	B	S
	NS	S	S	B	S	S
	NM	S	B	S	S	S
	NB	M	B	S	B	B

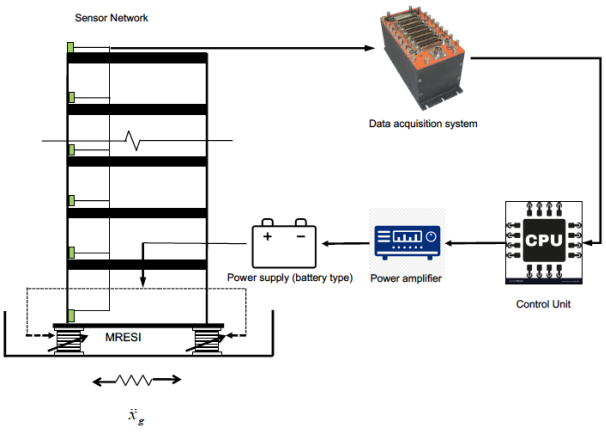

Fig. 12 Essential composition of a smart base isolation system

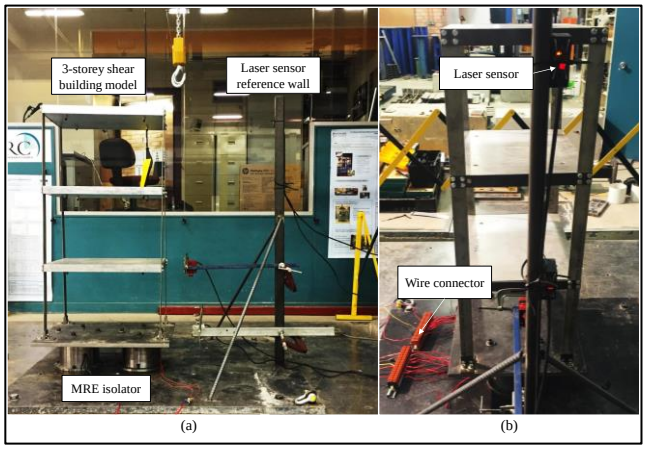

Fig. 13 Experimental setup of the smart base isolation system

accelerometers are the natural choice since in most cases other measurement feedbacks (such as displacement and velocity) are not accessible due to the moving reference during seismic event. In lab-based research, however, displacement sensors can be used. The data acquisition system collects the information of the building motion and sends them to the control unit for further processing. With built-in control algorithm, the control generates control command (usually 0-5V) to instruct the base isolator to act accordingly. The low-voltage control command needs to be amplified by the power amplifier and then input to the power supply. The smart base isolators located underneath the building require the DC power supply to drive the coil.

A small scaled testing scheme has been built under the umbrella of the smart base isolation system, as shown in Fig. 13. A three-storey building model is selected as the testing bed of the smart base isolation system. The testing building is a three-storey frame structure with a height of 1200 mm, of which each floor is 400 mm high. For computation efficiency, it is ideal that the system can be simplified as a lumped mass model.

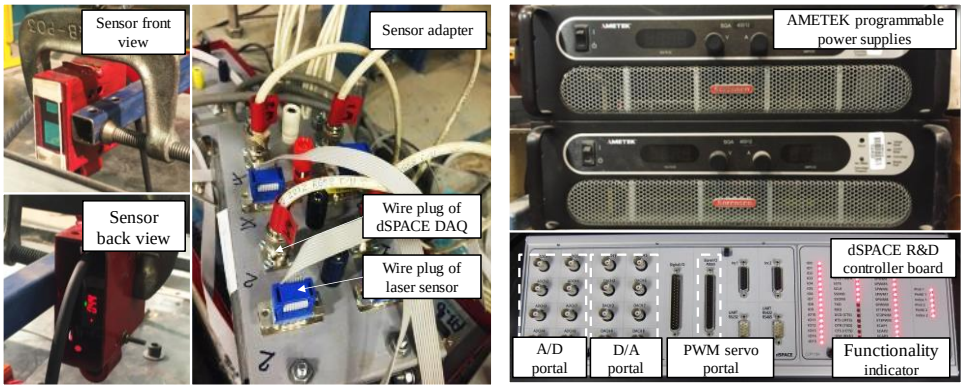

(a) (b)

Fig. 14 Sensor installation, power supply and control system: (a) Laser sensor and sensor adapter and (b) Power supplies and data acquisition system with dSPACE

Hence, this building model has been designed and manufactured as close to a pure shear model as possible. With such design, the likelihood of modal coupling of two directions is minimised and thus avoid the distortion of the building model. To achieve this objective, four identical steel strips, whose cross-section dimension is 34 mm × 4 mm, have been adopted as the columns of the structure to provide low stiffness at the direction of the earthquake excitation and very high stiffness at the perpendicular direction. Slab of each level consists of two aluminium plates with the dimension of 600 mm × 450 mm × 20 mm bolted together with four countersunk head screws. At connections at each floor, a steel clamp is bolted on the top of the strip with the mass plate, endowing the connection with high rigidity to avoid the occurrence of torsional and rotational modes.

In isolation scenarios, two MR elastomer base isolators are symmetrically mounted under the three-storey frame structure on the central axis of the structure's bottom plate. Hence, the equivalent mass of the isolation level is approximately 50 kg. In the passive isolation scenario, zero current is applied on the MRE isolator, which indicates the softest status of the isolator and thus the lowest corresponding natural frequency of the system.

A number of sensors are installed in this testing to measure the structure's movement feedback as well as the real-time current in the solenoid and magnetic field across the laminated MRE core of the isolator. Five Baumer laser distance sensors (Part No. OADM 20I4460/S14C) provide the measurements of shake table movement and relative displacement of each floor (only four are used in the fixed base building case). A sensor reference wall is built to hold the laser sensors precisely at the elevation of each floor. Sensors measuring 2nd and 3rd floors haves a sensing span of 130 mm while sensors measuring 1st and base floors as well as the table movement have a sensing span of 50 mm. Reason for this selection is that the bottom two floors and shake table feature relatively small displacement. Therefore, distance sensors with smaller measuring range can guarantee higher accuracy. Fig. 14(a) shows the photos of employed laser sensor and the adapter between sensing system and the data acquisition system. A Hall Effect current transducer (Part No. CSLA2CD) is utilised to monitor the real-time current I in the solenoid of MRE isolator. The magnetic flux B across the MRE core is measured by a digital Hall Effect sensor IC (Part No. SS461A). Two wire connectors are used for flexible configuration of small coils in MR elastomer isolators.

One of the essential equipment utilised in the control system is dSPACE Real-time PPC Controller Board (DS1104). This control board, based on MATLAB/Simulink operational interface, is a software-hardware platform for semi-physical simulation and can be installed in virtually any PC with a free PCI or PCIe slot. With dSPACE controller board, the PC can be upgraded to a powerful development system for rapid control prototyping, which is crucial in the realisation of real-time control of the smart base isolation system. The photo of dSPACE DS 1104 board is shown in Fig. 14(b). In the experimental system, the role of controller board functions comes in functional variants. First of all, it was employed as data acquisition system (DAQ). There are eight A/D converters and eight D/A converters on the board. Secondly, it also functions as a real-time controller based on Simulink software by generating the PWM control signal governing MR elastomer isolator at a switching frequency of 1000Hz. Seven out of eight A/D converters have been utilised to acquire feedback signals of five laser sensors, current transducer and Hall effect sensor. The control flow can be observed as following: the structural and shake table movement (x_g, x_b, x_1, x_2, x_3) as well as current and magnetic field (I and B) in MRE isolator are measured and transmitted to data acquisition system of dSPACE board; the inbuilt digital controller calculates desired control current and corresponding PWM signal; subsequently, the dSPACE board outputs command of duty cycle through PWM servo portal; according to the duty cycle, iGBT electrical switch aforementioned modulates the voltage applied on the MR elastomer isolator. Two AMETEK programmable power supplies (Sorensen SG Series, 400V/12A) in Fig. 14(b) have been employed to provide electricity.

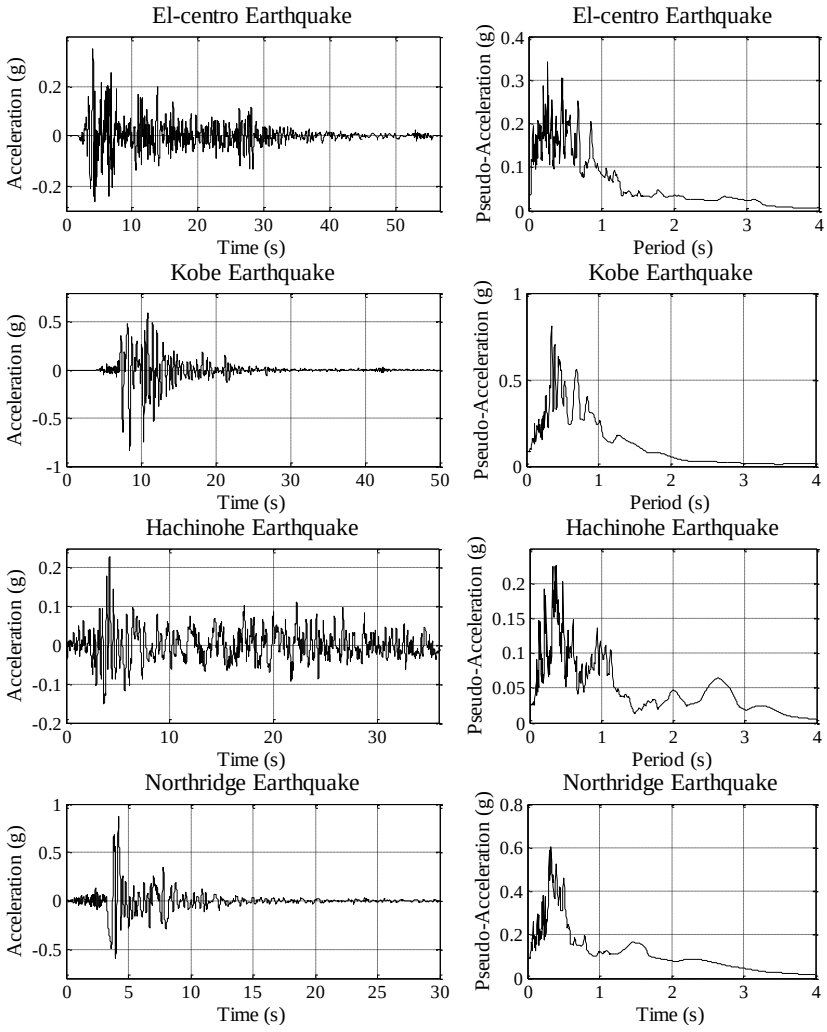

Fig. 14 Earthquake time histories and pseudo-acceleration spectra (damping ratio=5%)

3.5 Shake table testing of the smart base isolation system

Shake table is the essential step to testify the earthquake-proof of the proposed smart base isolation system. To appraise the seismic protection performance of the smart base isolation system under different control configurations, experimental testings are conducted under four natural acceleration records of historical earthquake events, namely, Imperial Valley 1940, Kobe 1995, Tokachi-Oki 1968, Northridge 1994. Selected from the databases of Pacific Earthquake Engineering Research Centre (PEERC) and National Geophysical Data Centre (NOAA-NGDG) [22], records of Imperial Valley (station: El Centro Array) and Tokachi-Oki (station: Hachinohe) earthquakes are categorised as far-fault earthquake, which features wider frequency range but longer excitation time while Kobe (station: KJMA) and Northridge (station: Sylmar) are classified as near-fault earthquakes which features waveforms containing large velocity pulses with lower frequency. Such selection consideration is capable of demonstrating the versatility of the proposed MRE base isolation system. The accelerograms and pseudo-acceleration spectrum (damping ratio is assumed as 5%) of the four earthquakes are shown in Fig. 15. From the time history records, long-period pulse-like waveforms can be clearly observed in Northridge earthquake. Meanwhile, pseudo-acceleration spectrums show that Kobe and Northridge earthquakes possesses larger acceleration spectra when the structural period is larger than 1s.

4. Perspectives on its future development

4.1 Performance evaluation

The performance of the proposed smart base isolation system is evaluated by comparing with building without base isolation, building with passive isolation system, smart base isolation system with on-off control and smart base isolation system with fuzzy logic control. Figs. 15 and 16 display the comparative time histories of top floor acceleration and base displacement of four isolation scenarios when subjected to four earthquakes. Comparatively, all isolated structures can effectively suppress the top floor acceleration over the entire time

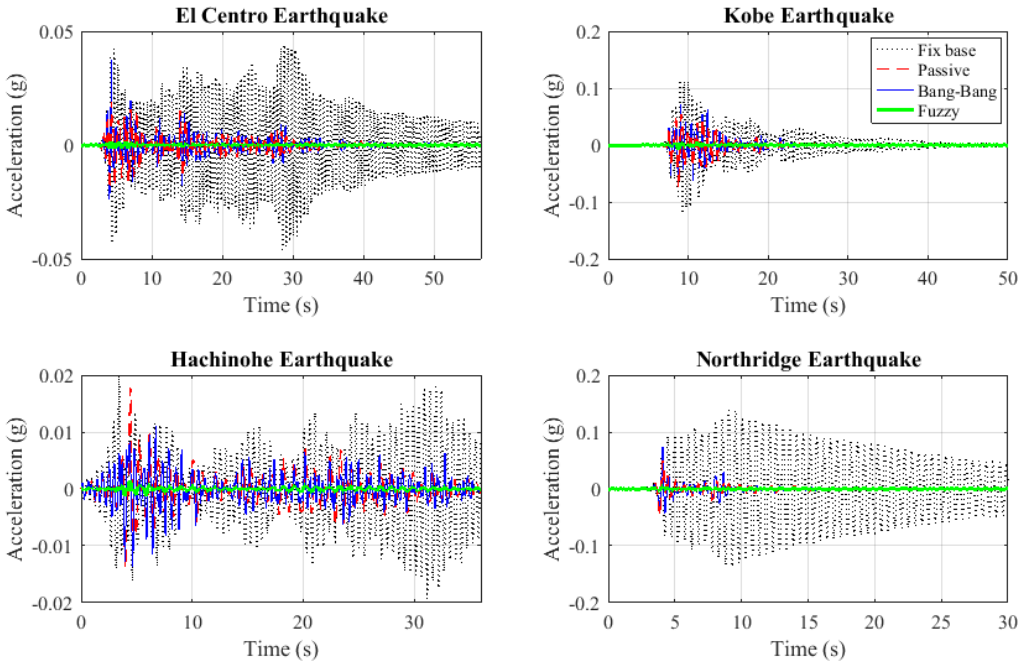

Fig. 15 Comparative time histories of top floor acceleration under four earthquakes

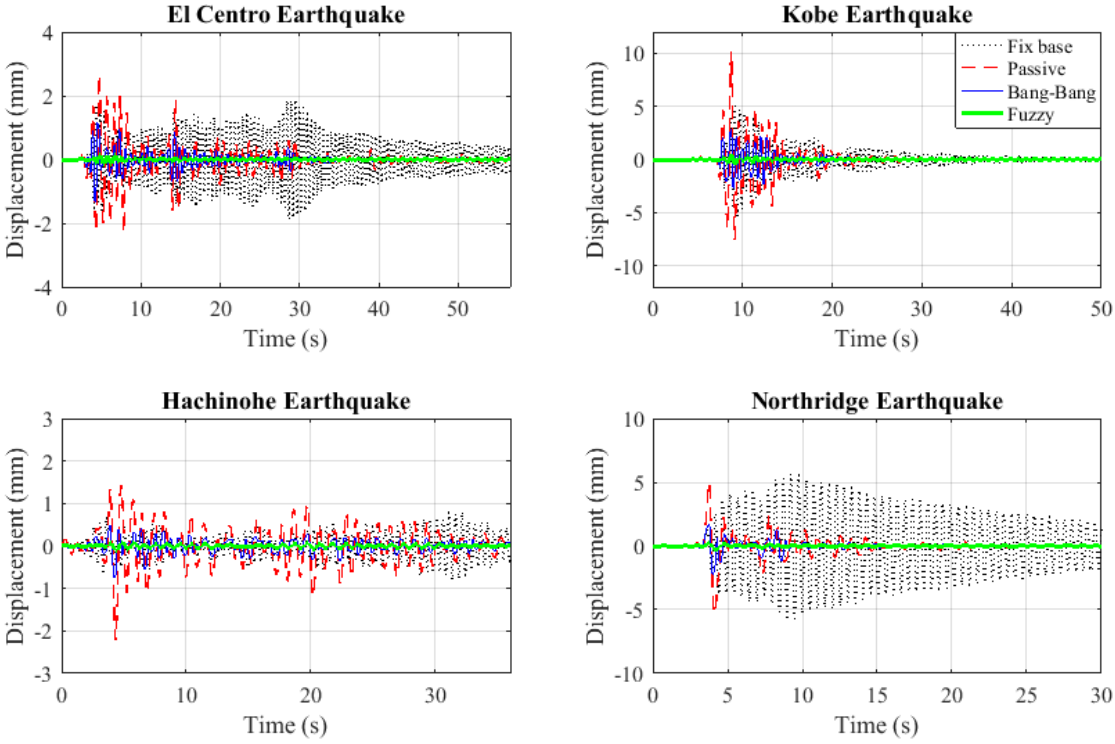

Fig. 16 Comparative time histories of base displacement under four earthquakes

history. As observed, under El Centro earthquake, there are three local excited acceleration peaks in the curve of passive isolation system. Under Kobe earthquake, the passive isolation system is intensively excited between 7 to 17 seconds and the peak acceleration occurs between 8 and 9 seconds. Under Hachinohe earthquake, the passive isolation system experienced the intense acceleration responses between 3 to 6 seconds and a re-excitation from

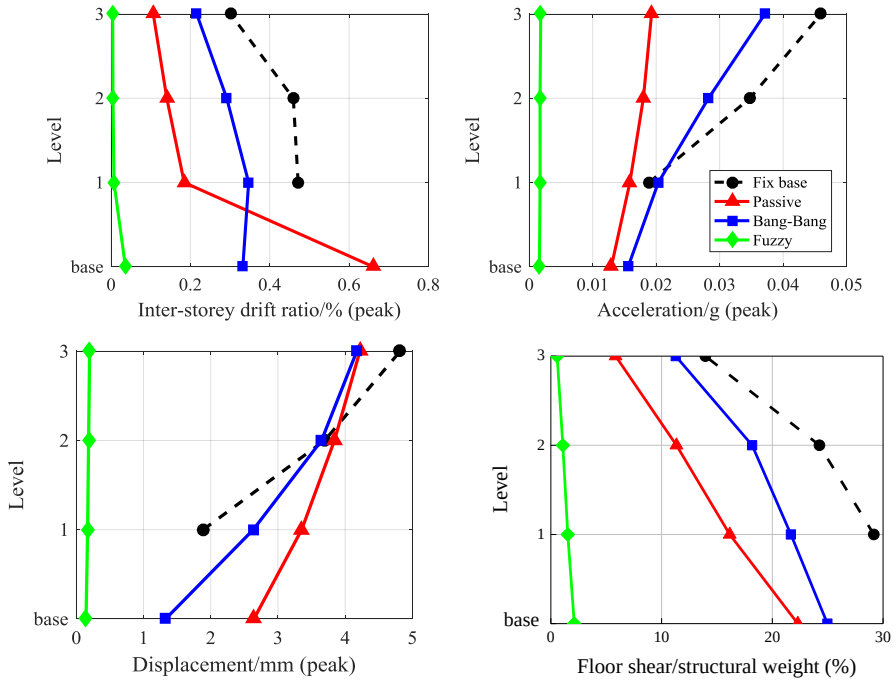

Fig. 17 Interstorey drift ratio (storey height: 400mm), peak floor acceleration, relative displacement and floor shear/seismic weight (fixed base building: 912.57N; baseisolated building: 1402.58N) under El Centro earthquake

the 12th second. It might be because, unlike other earthquakes, Hachinohe earthquake maintains a relatively high volatility until the end of the seismic event so disturbance continues. Hence, the disturbance continues in the Hachinohe earthquake.

Under Northridge earthquake, a wave-like acceleration pulse is observed in all isolation scenarios at around 3.5 to 4.5 seconds, which is caused by the near-fault feature of the seismic accelerogram. As Fig. 13 illustrates, the NFLC isolation system can not only effectively reduce the peak value of response but also maintain the acceleration at a low level throughout the entire earthquake excitation. The Bang-Bang controller, however, didn't achieve as good performance. As can be seen from Fig. 13, the acceleration response of Bang-Bang controller is close to that of the passive isolation system over the entire seismic event under Kobe and Hachinohe earthquake with a slightly smaller value and even surpassed the passive response under El Centro and Northridge earthquake, which suggests an inadequate capability in further acceleration reduction on the basis of a passive system.

The passive isolation system significantly amplified the base drift during 2~12s of El Centro earthquake, 7~15s of Kobe earthquake, 3~5s of Northridge earthquake and almost during the entire time history of Hachinohe earthquake. Under Kobe earthquake, the maximum base drift is almost 12mm, which is close to the threshold deformation of the MRE base isolator. Both of the controlled isolation system, however, performs well in suppressing the base drift. The NFLC controlled isolation system can dramatically reduce the displacement when compared with passive system, which indicates that controlled MRE base isolation system is an effective resolution to the issue of disproportionate base displacement happened in passive base isolation approaches.

Fig. 17 demonstrates the inter-storey drift ratio (compared with floor height), the peek floor acceleration, relative displacement and floor shear/seismic weight under the El-Centro Earthquake. As observed, the proposed smart base isolation system, whether using Bang-Bang control or fuzzy logic control, can all reduce the seismic response of the building very well. The fuzzy logic control can further reduce the structural response compared with Bang-Bang control, which enables a nearly rigid-body motion of the entire structure. It is due to the flexibility in the control signal where the Bang-Bang control jumps from maximum and minimum current, whilst the fuzzy logic control provides more fluidic and smooth transition of the control current. It not only reduces the bump of the structure but also can offers more non-resonant states of the structure when combating with earthquakes.

4.2 Challenges in future development

The idea of the smart base isolation system has been proposed and verified using a lab-scaled building model and the proposed smart base isolator. Although proven to be effective, the future development of such system featuring magnetorheological elastomer is yet to be optimistic, not until new advances in the material and control technology. It may face few challenges as followings:

- Material development: the MR elastomer used in this research is rather a soft rubber material which is not an application-ready material. With industrial rubber material as matrix, the MR effect will be

greatly reduced, quite contrary to the current 1630% increase in device stiffness. Based on the recent development, the MR effect using silicon rubber or natural rubber can reach a maximum 150% or less. Such range of stiffness change imposes more challenges in its device development.

- Device design: the current device has a diameter of 120 mm, measuring from the effective diameter of the elastomer pad. While the size of a normal rubber bearing may have the diameter of several meters. The substantial increase of the size creates more obstacle on the device design as the MR elastomer relies on an effective magnetic field to be energized. While a large coil will produce considerable heating issue during operation.
- Working mechanism: the current design of the device provides increasing lateral stiffness when a magnetic field is applied. The base isolation system prefers a low stiffness during seismic events. To be effectively working, the current design requires a constant magnetic field, thus energy input, during normal operational life, which is not economical and feasible. The negative stiffness changing MR elastomer isolator could be a solution while its effectiveness is yet to be proven.
- Asymmetric building: the building model used in the experimental testing is an idealized shear building with symmetric layout with the purpose to excite one dimensional motion. However, in the real world, no shear building can be easily found and buildings are always with asymmetric design (both geometric and mass distribution). It is expected that the torsional mode of the building will happen during seismic attacks. How to address this issue is fundamental critical.
- Practical issues: there are handful of practical issues to be considered, such as aging and stability of the material, code appliance of the isolator, acceptance from the community on the semi-active control, etc.

5. Conclusions

This paper overviews the recent development of a smart base isolation system for optimal seismic protection of civil structures. The concept of a smart base isolation system was proposed with interpolations on the necessary components and functionalities. A smart base isolation system should be able to realize the real-time decoupling of ground motion and thus provide optimal seismic protection to the structures under multiple types of earthquakes. To achieve the real-time decoupling, a base isolator with real-time controllable lateral stiffness should be developed. In light of this, the technological development of such system were presented, including the device design, nonlinear hysteresis modelling, structural control algorithm, system integration and experimental verifications. Finally, short comments on the development and the challenges ahead were discussed.

Acknowledgments

As the presented research was a team effort, the authors wish to acknowledge contributions from all members of their research team at Centre of Built Infrastructure Research, University of Technology Sydney, Australia. In particular, the authors wish to thank Dr Xiaoyu Gu for the work on the experimental realization of MRE adaptive isolation system, Dr Yang Yu for the work on MRE isolator modelling. The authors are also grateful to the helps from UTS laboratory staff, Peter Brown, Richard Turnell, Rami Haddad during the experimental research stage. In addition, the authors would like to acknowledge the financial supports on this research by Australian Research Council (DP150102636), Tianjin local government, China (Funding No.:18JCZDJC10010), and University of Technology Sydney in form of scholarship funding.

References

Behrooz, M., Wang, X. and Gordaninejad, F., (2014a), "Modeling of a new semi-active/passive magnetorheological elastomer isolator", *Smart Mater. Struct.*, **23**(4), 045013.

Behrooz, M., Wang, X. and Gordaninejad, F., (2014b), "Performance of a new magnetorheological elastomer isolation system", *Smart Mater. Struct.*, **23**(4), 045014.

Chen, L., Gong, X. and Li, W. (2007), "Microstructures and viscoelastic properties of anisotropic magnetorheological elastomers", *Smart. Mater. Struct.*, **16**(6), 2645.

Chen, S., Wang, X., Zhang, Z., Mu, W. and Li, R., (2016), "Optimal design of laminated-MRE bearings with multi-scale model", *Smart Mater. Struct*., **25** (10), 105037.

Chen, X., Li, J., Li, Y. and Gu, X. (2016), "Lyapunov-based semi-active control of structure with MRE base isolator", *Earthq. Struct*., **11**(6), 1077-1099.

Chen, X., Li, Y., Li, J. and Gu, X. (2018), "A novel dual-loop adaptive control for minimizing time response delay in real-time structural vibration control with magnetorheological (MR) devices", *Smart. Mater. Struct*., **27**(1), 015005.

Dyke, S.J., Spencer, B.F., Sain, M.K. and Carlson, J.D. (1996), "Modeling and control of magnetorheological dampers for seismic response reduction", *Smart. Mater. Struct*., **5**(5), 565.

Gu, X., Li, Y. and Li, J. (2016), "Investigations on response time of magnetorheological elastomer isolator for real-time control implementation", *Smart. Mater. Struct.*, **25**(11), 11LT03.

Gu, X., Yu, Y., Li, J. and Li, Y., (2017), "Semi-active control of magnetorheological elastomer base isolation system utilising learning-based inverse model", *J. Sound Vib*., **406**, 346-362 https://doi.org/10.1016/j.jsv.2017.06.023.

Gu, X., Yu, Y., Li, Y., Li, J., Askari, M. and Samali, B., (2019), "Experimental study of semi-active magnetorheological elastomer base isolation system using optimal neuro fuzzy logic control", *Mech. Syst. Signal Pr.*, **119**, 380-398. https://doi.org/10.1016/j.ymssp.2018.10.001.

Jangid, R. and Kelly, J.M. (2001), "Base isolation for near-fault motions", *Earthq. Eng. Struct. D.*, **30**(5), 691-707. https://doi.org/10.1002/eqe.31

Jung, H.J., Eem, S.H., Jang, D.D. and Koo, H.H. (2011), "Seismic Performance analysis of a smart base-isolation system considering dynamics of MR elastomer", *J. Intel. Mat. Syst. Str*., **22**(13), 1439-1450. https://doi.org/10.1177/1045389X11414224.

Kelly, J.M. (1999), "The role of damping in seismic isolation", *Earthq. Eng. Struct. D*., **28**(1), 3-20.

Kobori, T., Takahashi, M., Nasu, T, Niwa, N. and Ogasawara, K.

(1993), "Seismic response controlled structure with active variable stiffness system", *Earthq. Eng. Struct. D.*, **22**(11), 925-941. https://doi.org/10.1002/eqe.4290221102.

Koo, J. H., Khan, F., Jang, D.D. and Jung, H.H. (2009), "Dynamic characterization and modeling of magneto-rheological elastomers under compressive loadings", *Smart. Mater. Struct.*, **19**(11),117002.

Leng, D., Xu, K., Ma, Y., Liu, G. and Sun, L., (2018), "Modeling the behaviors of magnetorheological elastomer isolator in shear-compression mixed mode utilizing artificial neural network optimized by fuzzy algorithm (ANNOFA)", *Smart. Mater. Struct*., in press.

Li, J., Li, Y., Li, W. and Samali, B., (2013a), "Development of adaptive seismic isolators for ultimate seismic protection of civil structures", *Proc. SPIE 8692, Sensors and Smart Structures Technologies for Civil, Mechanical, and Aerospace Systems*.

Li, W.H., Zhou, Y. and Tian, T. (2010), "Viscoelastic properties of MR elastomers under harmonic loading", *Rheol. Acta*, **49**(7), 733-740.

Li, Y. and Li, J. (2015a), "Finite element design and analysis of adaptive base isolator utilizing laminated multiple magnetorheological elastomer layers", *J. Intel. Mat. Syst. Str.*, **26**(14), 1861-1870. https://doi.org/10.1177/1045389X15580654.

Li, Y. and Li, J. (2015b), "A highly-adjustable base isolator utilizing magnetorheological elastomer: experimental testing and modelling", *J. Vib. Acoust.*, **137**(1), 011009. doi: 10.1115/1.4027626.

Li, Y. and Li, J. (2017), "On rate-dependent mechanical model for adaptive magnetorheological elastomer base isolator", *Smart. Mater. Struct.*, **26**(4), 045001.

Li, Y., Li, J. and Samali, B. (2012), "A novel adaptive base isolator utilising magnetorheological elastomer", *Proceedings of the 22nd Australasian Conference on the Mechanics of Structures and Materials*, Sydney, Australia, 11-14 December.

Li, Y., Li, J. and Samali, B. (2013d), "On the magnetic field and temperature monitoring of a solenoid coil for a novel magnetorheological elastomer base isolator", *J. Phys. Conf. Ser.* **412**(1), 012033

Li, Y., Li, J., Li, W. and Du, H. (2014), "A state-of-the-art review on magnetorheological elastomer devices", *Smart. Mater. Struct*., **23**(12), 123001.

Li, Y., Li, J., Li, W. and Samali, B. (2013b), "Development and characterization of a magnetorheological elastomer based adaptive seismic isolator", *Smart Mater. Struct.*, **22(**3), 035005.

Li, Y., Li, J., Tian, T. and Li, W., (2013c), "A highly adjustable magnetorheological elastomer base isolator for applications of real-time adaptive control", *Smart Mat. Struct.*, **22(**9), 095020.

Lu, L. Y., Lin, G.L. and Lin, C.Y. (2011), "Experiment of an ABS-type control strategy for semi-active friction isolation systems", *Smart Struct. Syst*., **8**(5), 501-524. http://dx.doi.org/10.12989/sss.2011.8.5.501.

Lu, L.Y. and Lin, G.L. (2009), "Fuzzy friction controllers for semi-active seismic isolation systems", *J. Intel. Mat. Syst. Str*., **20**(14), 1747-1770. https://doi.org/10.1177/1045389X09343788.

Makris N. (1997), "Rigidity-plasticity-viscosity: can electorheological dampers protect base-isolated structuers from near-source ground motions?", ,*Earthq. Eng. Struct. D.*, **26**(5), 57-591

Nagarajaiah, S. and Narasimhan, S. (2006), "Smart base-isolated benchmark building. Part II: Phase I sample controllers for linear isolation systems", *Struct. Control Health Monit.*, **13**(2-3), 589-604. https://doi.org/10.1002/stc.100.

Narasimhana S. and Nagarajaiah S. (2005), "A STFT semiactive controller for base isolated buildings with variable stiffness isolation systems", *Eng. Struct*., **27**(4), 514-523 https://doi.org/10.1016/j.engstruct.2004.11.010.

Ozbulut, O.E. and Silwal, B. (2016), "Performance assessment of buildings isolated with S-FBI system under near-fault earthquakes", *Smart Struct. Syst*., **17**(5), 709-724.

Tiong, P.L.Y., Kelly, J.M. and Or, T.T. (2017), "Design approach of high damping rubber bearing for seismic isolation", *Smart Struct. Syst*., **20**(3), 303-309.

Usman, M., Sung, S.H., Jang, D.D., Jung, H.J. and Koo, J.H., (2009), "Numerical investigation of smart base isolation system employing MR elastomer", *J. Phys. Conf. Ser.*, **149**(1), 012099.

Yang, J., Du, H., Li, W., Li, Y., Li, J., Sun, S. and Deng, H. (2013), "Experimental study and modeling of a novel magnetorheological elastomer isolator", *Smart Mater. Struct*., **22**(11), 117001.

Yi, F., Dyke S.J., Caicedo, J.M and Carlson, J.D. (2001), "Experimental verification of multiinput seismic control strategies for smart dampers", *J. Eng. Mech*., **127**(11), 1152-1164. https://doi.org/10.1061/(ASCE)0733-9399(2001)127:11(1152).

Yoshida, O. and Dyke, S.J. (2004), "Seismic control of a nonlinear benchmark building using smart dampers", *J. Eng. Mech.*, **130** (4), 386-392. https://doi.org/10.1061/(ASCE)0733-9399(2004)130:4(386).

Yoshioka, H., Ramallo, J. and Spencer, B.F. (2002), "Smart base isolation strategies employing magnetorheological dampers", *J. Eng. Mech*., **128**(5), 540-551. https://doi.org/10.1061/(ASCE)0733-9399(2002)128:5(540).

Yu, Y., Li, Y. and Li, J. (2014), "Parameter identification of an improved Dahl model for magnetorheological elastomer base isolator based on enhanced Genetic algorithm", *Proceedings of the 23rd Australasian Conference on the Mechanics of Structures and Materials*, Byron Bay, Australia, 9-12 December 2014.

Yu, Y., Li, Y. and Li, J. (2015a), "Parameter identification of a novel strain stiffening model for magnetorheological elastomer base isolator utilizing enhanced particle swarm optimization", *J. Intel. Mat. Syst. Str.*, **26**(18), 2446-2462. https://doi.org/10.1177/1045389X14556166.

Yu, Y., Li, Y. and Li, J. (2015b), "Parameter identification and sensitivity analysis of an improved LuGre friction model for magnetorheological elastomer base isolator", *Meccanica*, **50** (11), 2691-2707.

Yu, Y., Li, Y. and Li, J. (2015c), "Nonparametric modeling of magnetorheological elastomer base isolator based on artificial neural network optimized by ant colony algorithm", *J. Intel. Mat. Syst. Str.*, **26**(14), 1789-1798 https://doi.org/10.1177/1045389X15577649.

Yu, Y., Li, Y., Li, J. and Gu, X., (2016a), "A novel hysteresis model for dynamic behaviour of magnetorheological elastomer base isolator", *Smart. Mater Struct*., **25** (5), 055029.

Yu, Y., Li, Y., Li, J. and Gu, X. (2016b), "Self-adaptive step fruit fly algorithm optimized support vector regression model for dynamic response prediction of magnetorheological elastomer base isolator", *Neurocomputing*, **211**, 41-52. https://doi.org/10.1016/j.neucom.2016.02.074.

Yu, Y., Sayed, R., Li, J., Li, Y. and Ha, Q. (2016c), "Magnetorheological elastomer base isolator for earthquake response mitigation on building structures: modeling and second-order sliding mode control", *Earthq. Struct.*, **11**(6), 943-966. http://dx.doi.org/10.12989/eas.2016.11.6.943.

Zeng, J., Guo, Y., Li, Y., Zhu, J. and Li, J., (2013), "Two-dimensional magnetic property measurement for magneto-rheological elastomer", *J. Appl. Phys.*, **113**(17), 17A919. https://doi.org/10.1063/1.4796046.